Electronic Supplementary Material (ESI) for Journal of Materials Chemistry A.

Supporting Information

Polyoxometalate-based metal-organic framework-derived hybrid electrocatalysts for highly efficient hydrogen evolution reaction

Ji-Sen Li,[a,b] Yu-Jia Tang,[a] Chun-Hui Liu,[a] Shun-Li Li,[a] Run-Han Li,[a] Long-Zhang Dong,[a] Zhi-Hui Dai,*[a] Jian-Chun Bao,[a] and Ya-Qian Lan*[a]

[a]School of Chemistry and Materials Science, Nanjing Normal University, Nanjing 210023, P. R. China

[b]Key Laboratory of Inorganic Chemistry in Universities of Shandong, Department of Chemistry and Chemical Engineering, Jining University, Qufu, 273155, Shandong, P. R. China.

*E-mail: yqlan@njnu.edu.cn; daizhihuii@njnu.edu.cn

S1. Materials and Preparation of the catalysts

All reagents were analytical grade and used without further purification. All solutions used in electrochemical experiments were prepared with Millipore water (≥18 MΩ).

Synthesis of MIL-100 (Fe)

MIL-100 (Fe) was prepared following the protocol described earlier.[1] In a typical synthesis, 5 mL of water solution consisting of $FeCl_3 \cdot 6H_2O$ (162.2 mg), and trimethyl 1,3,5-benzenetricarboxylate (138.7 mg) were thoroughly dissloved with ultrasonication. Subsequently, the solution was heated at 130 °C for 72 h in a Teflon reactor. The resulting brown solids were isolated by centrifuging, and were washed with acetone.

Synthesis of PMo12@MIL-100 (Fe)

50 mL of water solution consisting of $FeCl_3 \cdot 6H_2O$ (1.89 g), and $H_3PMo_{12}O_{40}$ (3.15 g) were thoroughly dissloved with ultrasonication. Then, trimethyl 1,3,5-benzenetricarboxylate (1.36 g) was added into the above solution. Subsequently, the solution was heated at 130 °C for 72 h in a Teflon reactor. The resulting brown solids were isolated by centrifuging, and were washed with ethanol and ether.

Synthesis of Fe_3C/Mo_2C@NPGC

1 g of PMo12@MIL-100 (Fe) and 1g of melamine were mixed by ball milling. And then, the mixture was pyrolyzed in a flow of ultrapure N_2 at different temperatures (700, 900, and 1100 °C) for 5 h with the heating rate of 5 °C min^{-1}. The obtained samples were acid etched in H_2SO_4 (0.5 M) by 24 h of continuous agitation at 80 °C to remove unstable and inactive species. The etched samples were then thoroughly washed with de-ionized water until reaching a neutral pH, and defined as Fe_3C/Mo_2C@NPGC-700, Fe_3C/Mo_2C@NPGC-900 (Fe_3C/Mo_2C@NPGC), and Fe_3C/Mo_2C@NPGC-1100, respectively.

Synthesis of Fe_3C@C

1 g of MIL-100 (Fe) was pyrolyzed in a flow of ultrapure N_2 at 900 °C for 5 h with the heating rate of 5 °C min^{-1}. The obtained samples were acid etched in H_2SO_4 (0.5 M) by 24 h of continuous agitation at 80 °C to remove unstable and inactive species. The etched samples were then thoroughly washed with de-ionized water until reaching a neutral pH, and defined as Fe_3C@C.

Synthesis of Fe_3C/FeMo/Mo_2C

1 g of PMo12@MIL-100 (Fe) was pyrolyzed in a flow of ultrapure N_2 at 900 °C for 5 h with the heating rate of 5 °C min^{-1}. The obtained samples were acid etched in H_2SO_4 (0.5 M) by 24 h of continuous agitation at 80 °C to remove unstable and inactive species. The etched samples were then thoroughly washed with de-ionized water until reaching a neutral pH, and

defined as $Fe_3C/FeMo/Mo_2C$.

Characterizations

The transmission electron microscopy (TEM) and high-resolution TEM (HRTEM) images were recorded on JEOL-2100F apparatus at an accelerating voltage of 200 kV. Surface morphologies of the carbon materials were examined by a scanning electron microscope (SEM, JSM-7600F) at an acceleration voltage of 10 kV. The energy-dispersive X-ray spectroscopy (EDS) was taken on JSM-5160LV-Vantage typed energy spectrometer. The powder X-Ray diffraction (XRD) patterns were recorded on a D/max 2500VL/PC diffractometer (Japan) equipped with graphite monochromatized Cu Kα radiation (λ = 1.54060 Å). Corresponding work voltage and current is 40 kV and 100 mA, respectively. X-ray photon spectroscopy (XPS) was recorded by a scanning X-ray microprobe (PHI 5000 Verasa, ULAC-PHI, Inc.) using Al kα radiation and the C1s peak at 284.8 eV as internal standard. The Raman spectra of dried samples were obtained on Lab-RAM HR800 with excitation by an argon ion laser (514.5 nm). The nitrogen adsorption-desorption experiments were operated at 77 K on a Micromeritics ASAP 2050 system. The pore size distributions were measured by Barret-Joyner-Halenda (BJH) model. Prior to the measurement, the samples were degassed at 150 ^{o}C for 10 h.

Electrochemical Measurements

All electrochemical experiments were conducted on a CHI 760 D electrochemical station (Shanghai Chenhua Co., China) in a standard three electrode cell in 0.5 M H_2SO_4 at room temperature. A glassy carbon electrode (GCE, 3 mm in diameter), an Ag/AgCl with saturated KCl, and a Pt wire were used as the working electrode, reference and counter electrode, respectively. 4 mg of the catalysts were dispersed in 2 mL of 9:1 v/v water/Nafion by sonication to form a homogeneous ink. Typically, 5 μL well-dispersed catalysts were covered on the glassy carbon electrode and then dried in an ambient environment for measurements. The electrocatalyst was prepared with a catalyst loading of 0.14 mg cm^{-2}. Commercial 20% Pt/C catalyst was also used as a reference sample. Linear sweep voltammetry (LSV) was tested with a scan rate of 5 mV s^{-1}. Electrochemical impedance spectroscopy (EIS) measurements were carried out from 1000 kHz to 100 mHz with an amplitude of 10 mV at the open-circuit voltage. The electrochemical stability of the catalyst was conducted by cycling the potential between -0.3 and 0.3 V vs RHE at a scan rate of 100 mV s^{-1}. The Chronoamperometry (CA) were tested at an overpotential of -0.12 V vs RHE after equilibrium. To estimate the electrochemical active surface areas of the catalysts, cyclic voltammograms (CV) was tested by measuring double-layer capacitance (EDLC) under the potential window of 0.19 – 0.39 V vs RHE with various scan rate (20, 40, 60, 80, 100, 120, 140, 160, 180, and 200 mV s^{-1}). A flow of N_2 was maintained over the electrolyte during the experiment to eliminate dissolved oxygen. The potential vs RHE was converted to the reversible hydrogen electrode (RHE) via the Nernst equation: $E_{\mathrm{RHE}} = E_{\mathrm{Ag/AgCl}} + 0.059\ \mathrm{pH} + E^{\theta}_{\mathrm{Ag/AgCl}}$. In 0.5 M H_2SO_4, $E_{\mathrm{RHE}} = 0.21\ \mathrm{V} + E_{\mathrm{Ag/AgCl}}$.

(1) Canioni R., Roch-Marchal C., Secheresse F., Horcajada P., Serre C., Hardi-Dan M., Ferey G., Greneche J.-M., Lefebvre F., Chang J.-S., Hwang Y.-K., Lebedev O., Turner S. and Tendeloo G. Van, *J. Mater. Chem.* **2011**, *21*, 1226-1233.

S2. Figures in Supporting Information

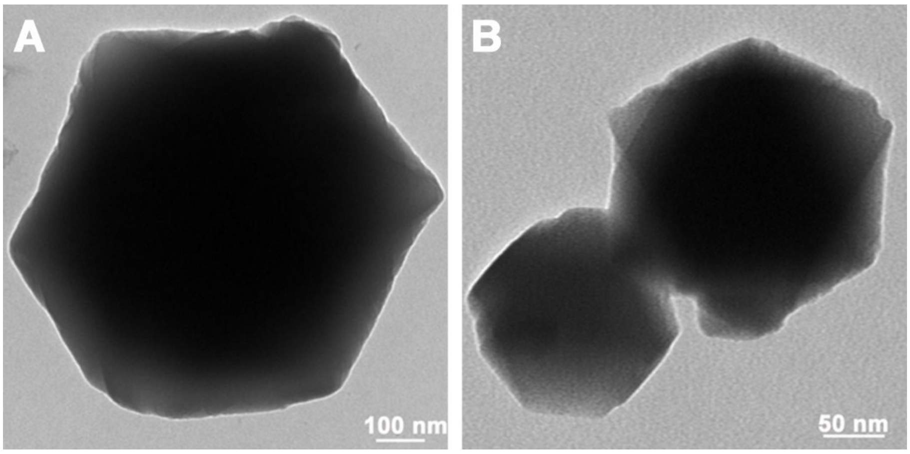

Fig. S1 TEM of MIL-100 (Fe) and PMo_{12}@MIL-100 (Fe)

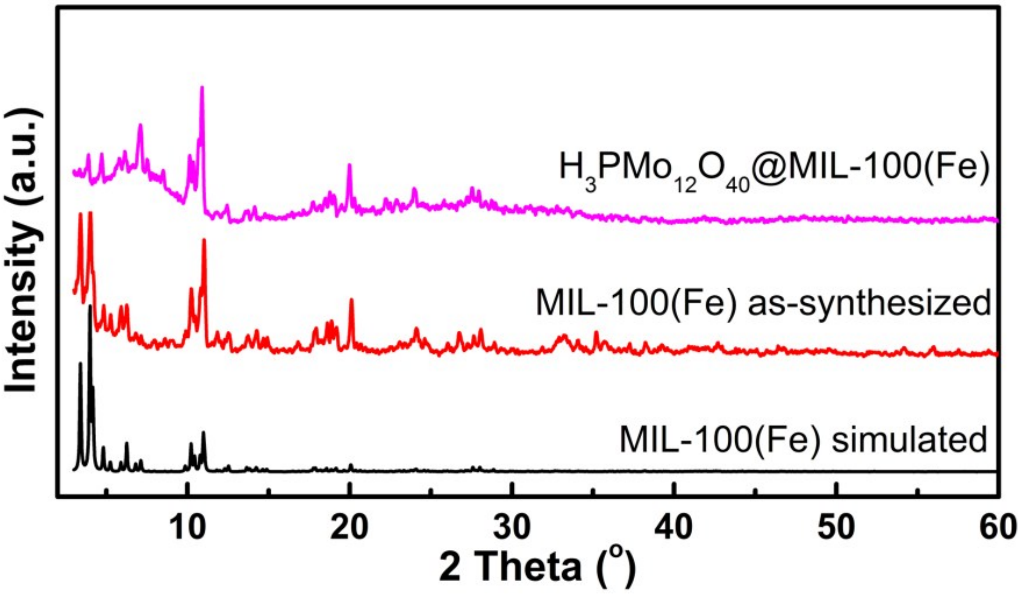

Fig. S2 XRD of MIL-100 (Fe), $H_3PMo_{12}O_{40}$@MIL-100 (Fe), and MIL-100 (Fe) simulated, respectively.

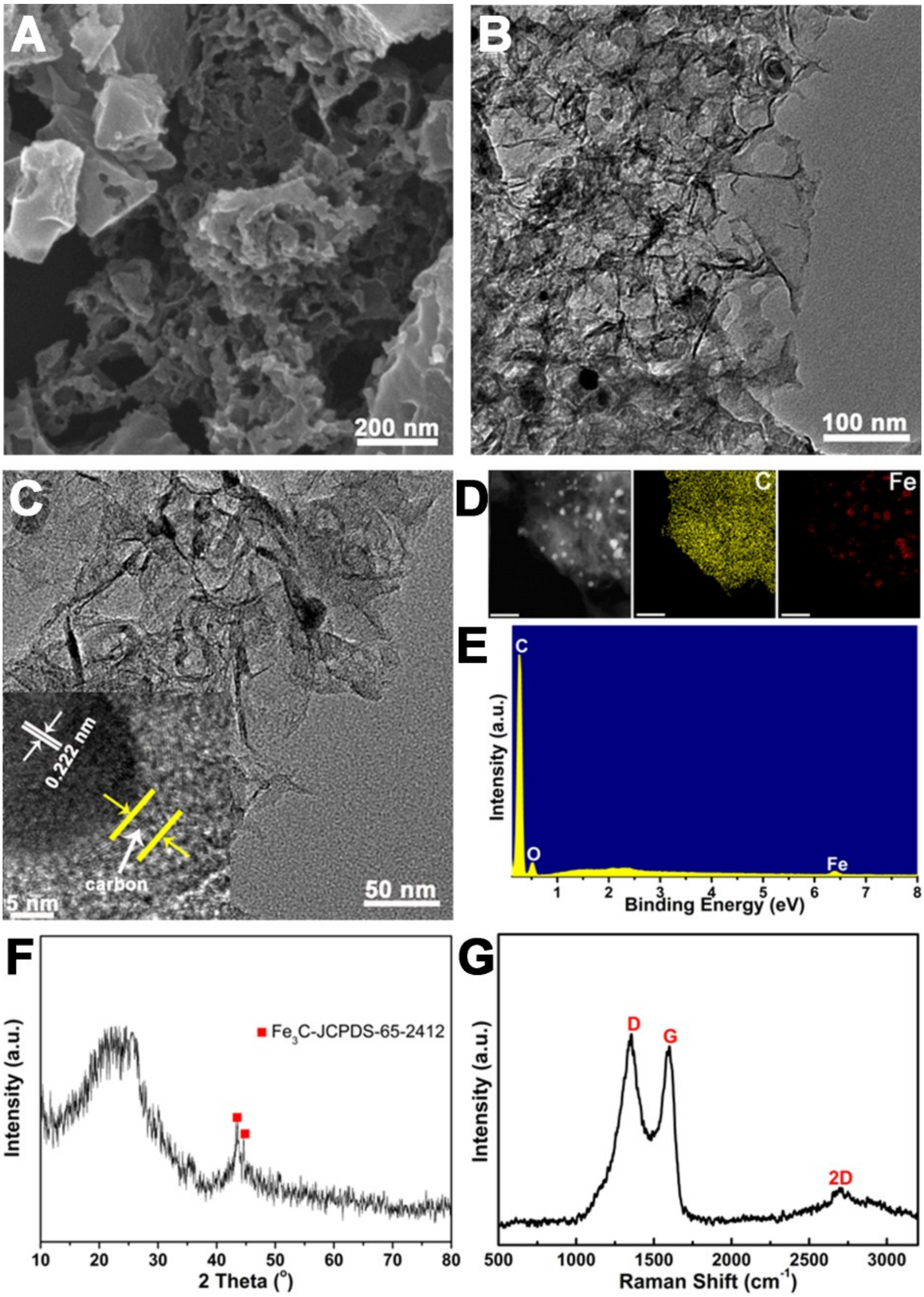

Fig. S3 Typical SEM image (A), low and high magnification TEM images (B-C), STEM image and EDX elemental mapping of C, Mo, Fe, N, and P (D), scale bar 50 nm. EDS spectrum (E), XRD pattern (F), and Raman spectrum (G) of $Fe_3C@C$.

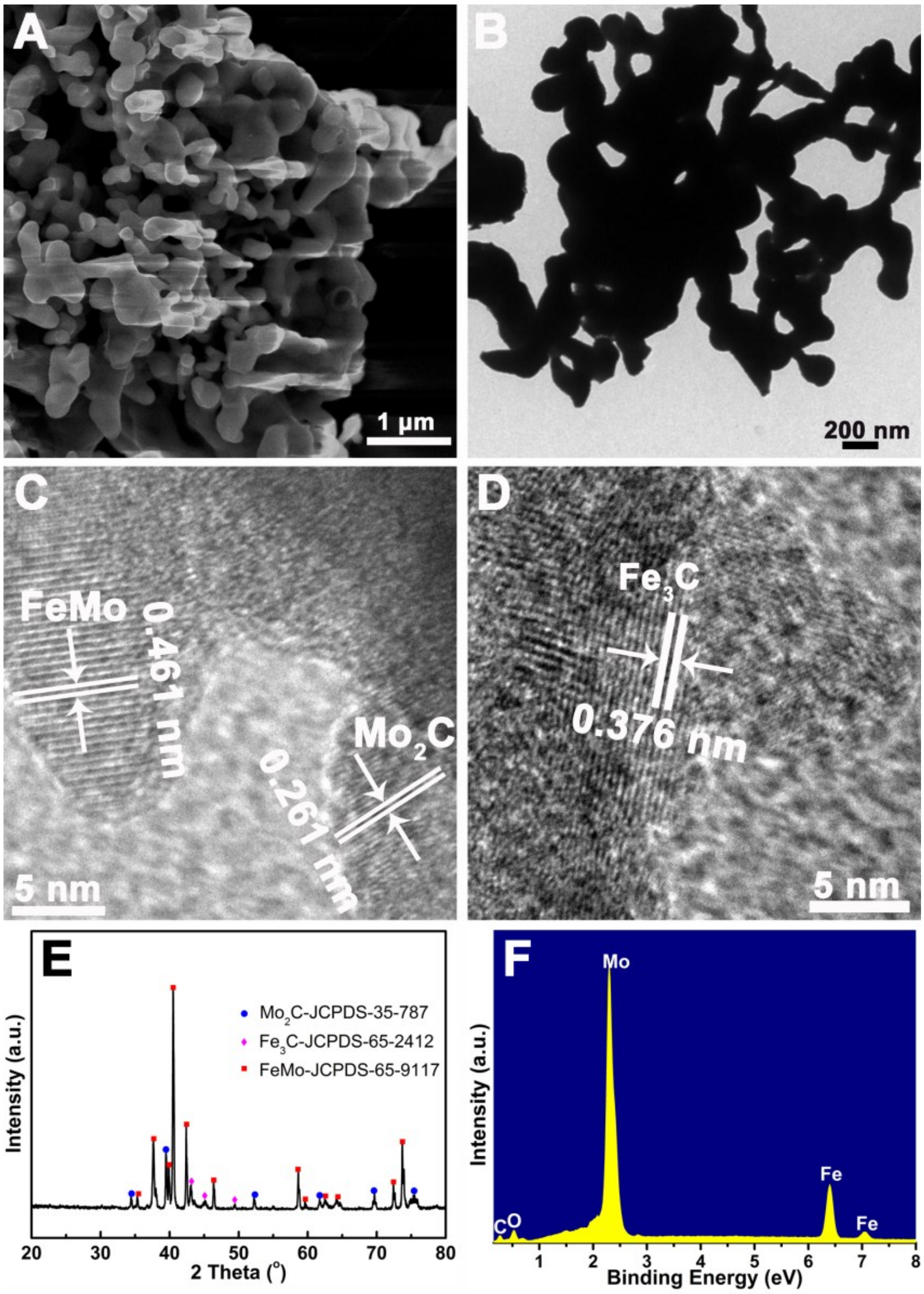

Fig. S4 Typical SEM image (A), TEM image (B), HRTEM images (C-D), XRD pattern (E), and EDS spectrum (F) of Fe_3C/FeMo/Mo_2C.

SEM and TEM images of Fe_3C@C (Fig. S3A-C) show that a handful of nanoparticles are distributed on the porous carbon. From the inset of Figure S3C, the Fe_3C (201) plane can be obviously seen with a lattice spacing of 0.222 nm. The element mapping images are shown in Fig. S3D, clearly revealing the Fe_3C@C catalyst consists of C and Fe, which is consistent with that of EDS (Fig. S3E). The crystalline phase of Fe_3C@C characterized by PXRD is illustrated in Figure S3F. The peaks located at 43.5, and 44.7 ^{o} are indexed to the (201), and (211) planes of Fe_3C (JCPDS-65-2412), respectively. Fig. S3G exhibits the Raman spectrum of Fe_3C@C. Due to the absence of melamine, the corresponding graphitic degree of Fe_3C@C is lower than that of Fe_3C/Mo_2C@NPGC. On the other hand, the morphology and crystal structure of $Fe_3C/FeMo/Mo_2C$ were also examined, similar to $Fe_3C@C$. However, it is found that nanoparticles are aggregated together and no porous carbon is existent (Fig. S4A-B). From HRTEM images (Fig. S4C-D), the lattice spacings of 0.376, 0.461, and 0.261 nm, are assigned to the (011) plane of Fe_3C, (200) plane of FeMo, and (100) plane of Mo_2C. PXRD pattern indicates that the peaks at 34.4, 39.4, 52.2, 61.7, 69.7, and 75.4 ° ascribed to (100), (101), (102), (110), (103), and (202) planes of Mo_2C (JCPDS-35-787). The peaks around 43.1, 44.9 and 43.78 ° arise from Fe_3C (JCPDS-65-2412). The additional peaks are assigned to FeMo (JCPDS-65-9117). Figure S4F demonstrates the EDS spectrum, verifying the existence of Fe, Mo, and C.

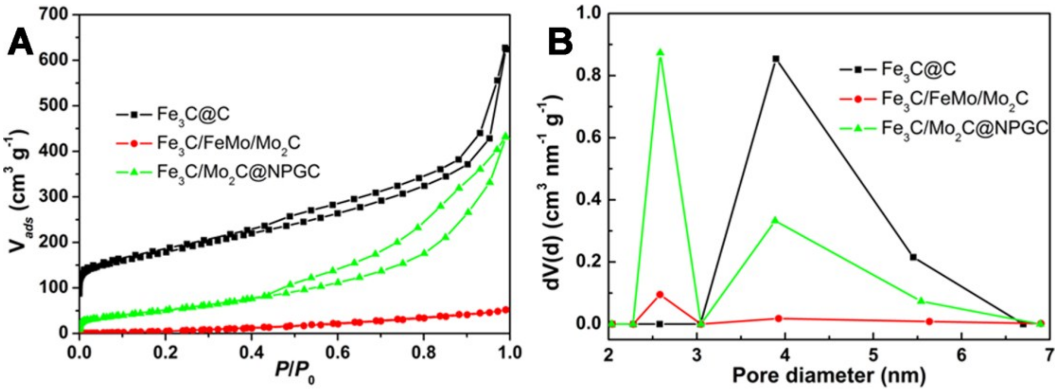

Fig. S5 N_2 adsorption-desorption isotherms (A) and pore size distributions (B) of different samples by BJH model.

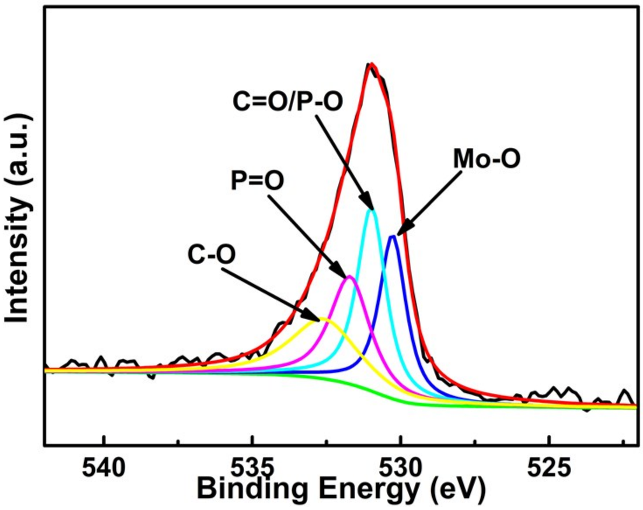

Fig. S6 High-resolution scans of O 1s electrons of $Fe_3C/Mo_2C@NPGC$.

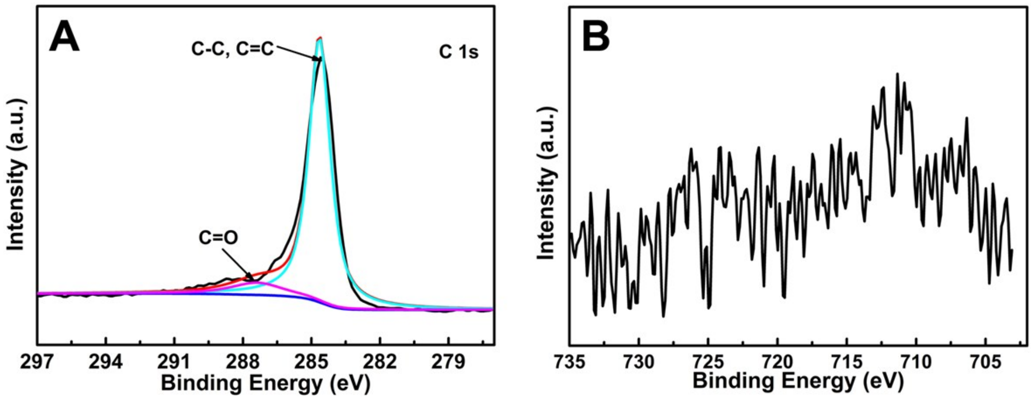

Fig. S7. (A-B) High-resolution scans of C 1s, and Fe 2p electrons of $Fe_3C@C$.

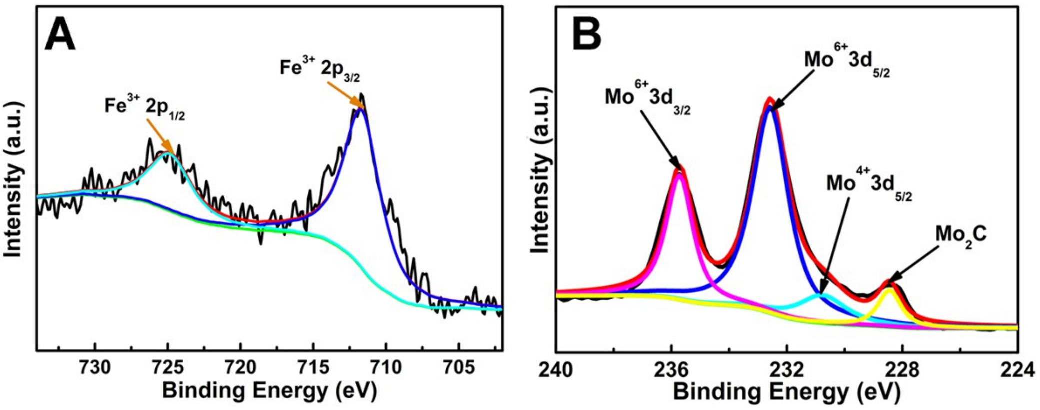

Fig. S8 (A-B) High-resolution scans of Fe 2p and Mo 3d electrons of $Fe_3C/FeMo/Mo_2C$.

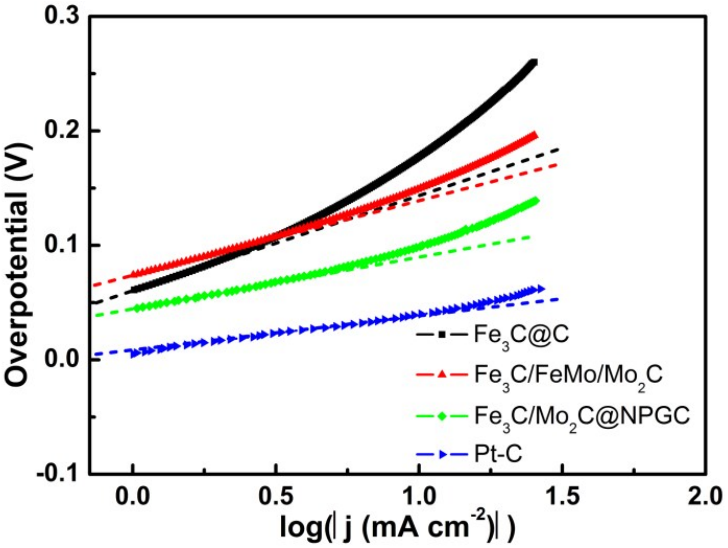

Fig. S9 Calculation of exchange current density of different samples.

Tafel plot is fit into the Tafel equation (η = b log (j) + a, where b is the Tafel slope). The corresponding exchange current density (j_0) was calculated by extrapolation methods when $\eta = 0$ V.

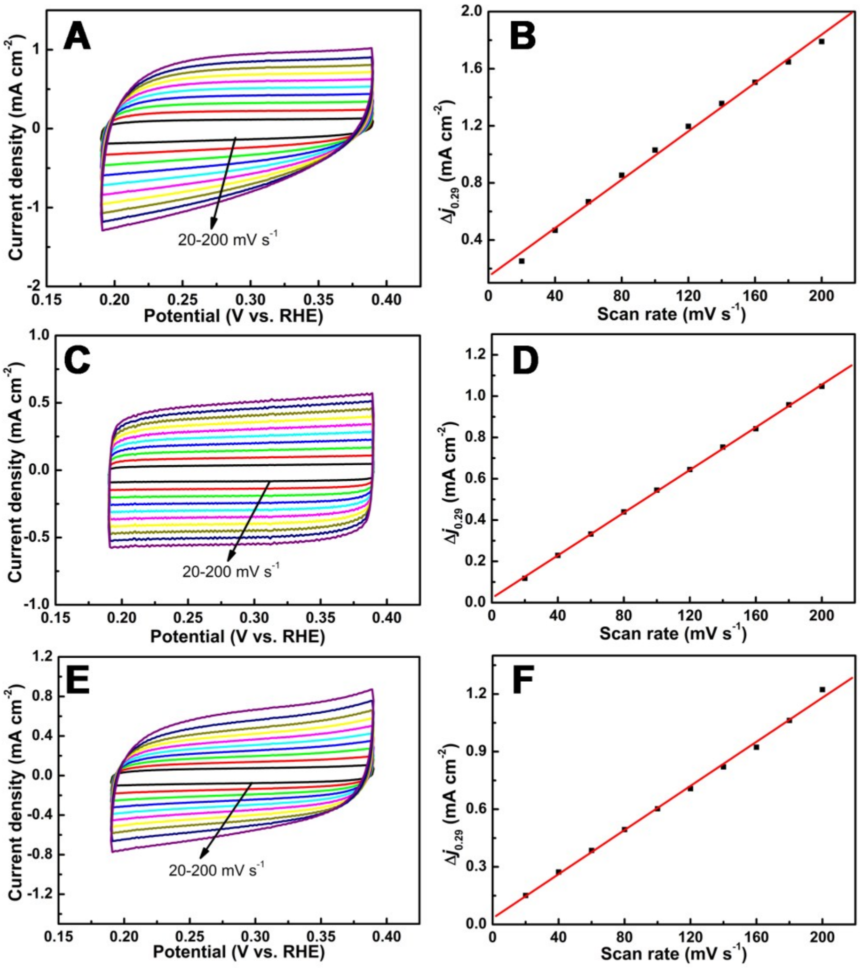

Fig. S10 Cyclic voltammetrys of (A) Fe_3C@C, (C) $Fe_3C/FeMo/Mo_2C$, and (E) Fe_3C/Mo_2C@NPGC. (B, D, F) The corresponding capacitive currents at 0.29 V as a function of scan rate for Fe_3C@C, $Fe_3C/FeMo/Mo_2C$, and Fe_3C/Mo_2C@NPGC.

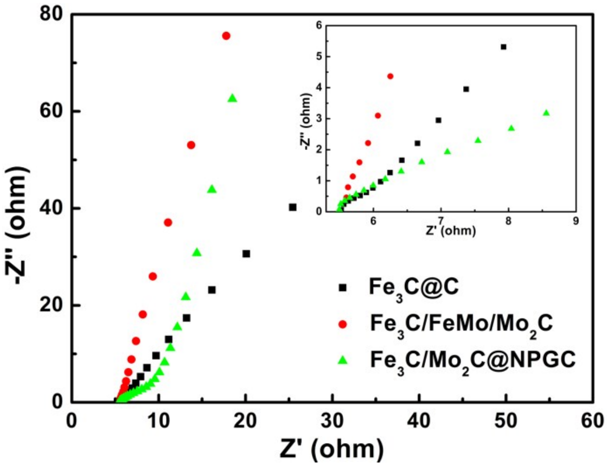

Fig. S11 Electrochemical impedance spectra (EIS) of three electrocatalysts over the frequency ranging from 1000 kHz to 0.1 Hz at the open-circuit voltage. Inset denotes the magnified images of high frequency region.

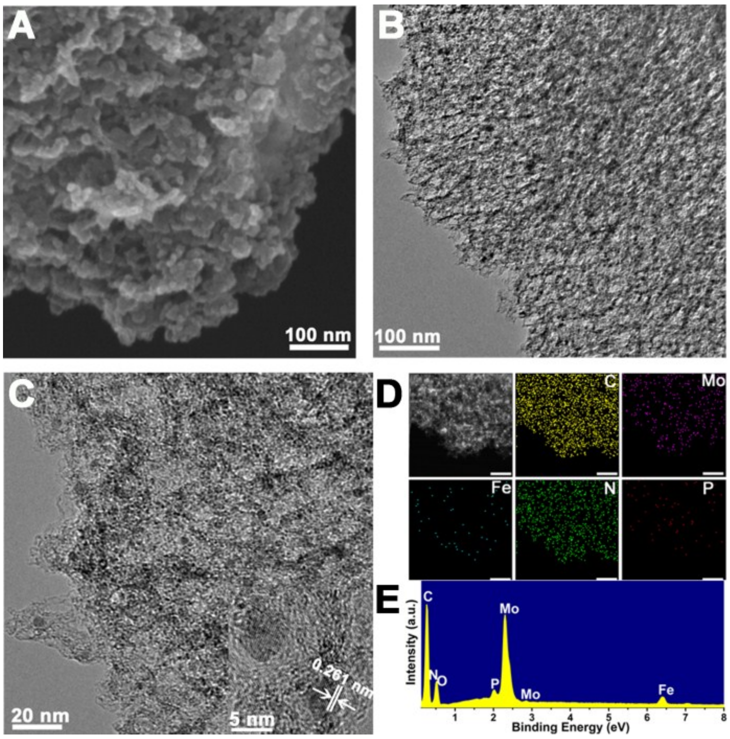

Fig. S12 Typical SEM image (A) low and high magnification TEM images (B-C), STEM image and EDX elemental mapping of C, Mo, Fe, N, and P (D), scale bar 50 nm, EDS spectrum (E) of Fe_3C/Mo_2C@NPGC (700 ^oC).

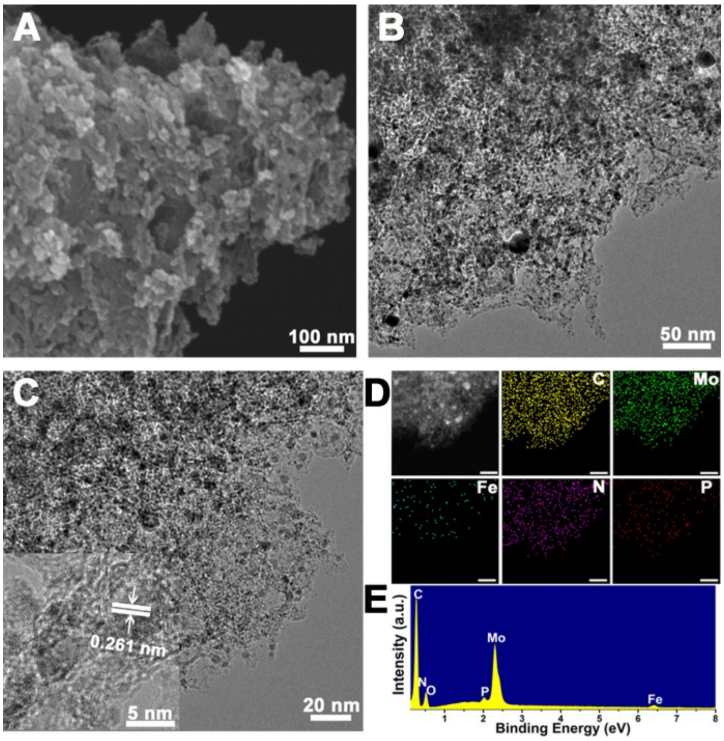

Fig. S13 Typical SEM image (A), low and high magnification TEM images (B-C), STEM image and EDX elemental mapping of C, Mo, Fe, N, and P (D), scale bar 50 nm. EDS spectrum (E), of Fe_3C/Mo_2C@NPGC (1100 ^oC).

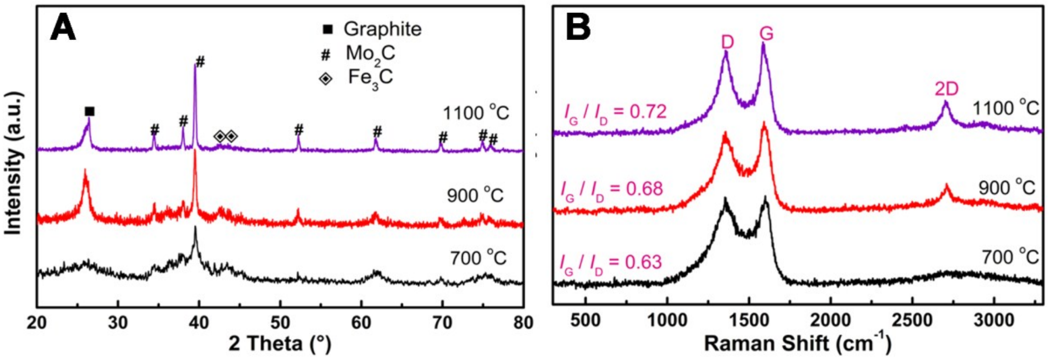

Fig. S14 XRD patterns (A), and Raman spectra (B) of Fe_3C/Mo_2C@NPGC carbonized at 700, 900, and 1100 °C, respectively.

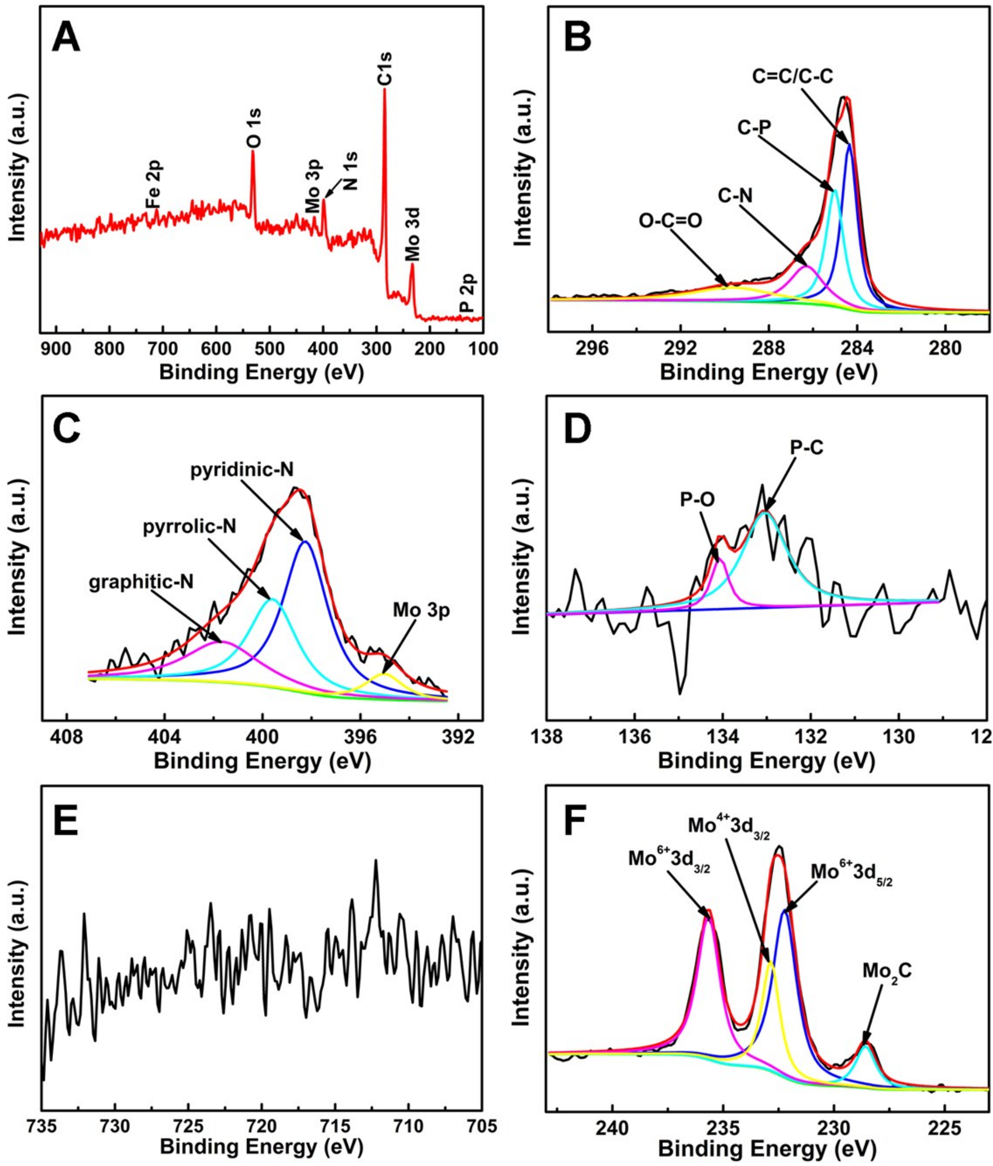

Fig. S15 (A-F) XPS survey spectra and high-resolution scans of C 1s, N 1s, P 2p, Fe 2p, and Mo 3d electrons of Fe_3C/Mo_2C@NPGC (700 °C), respectively.

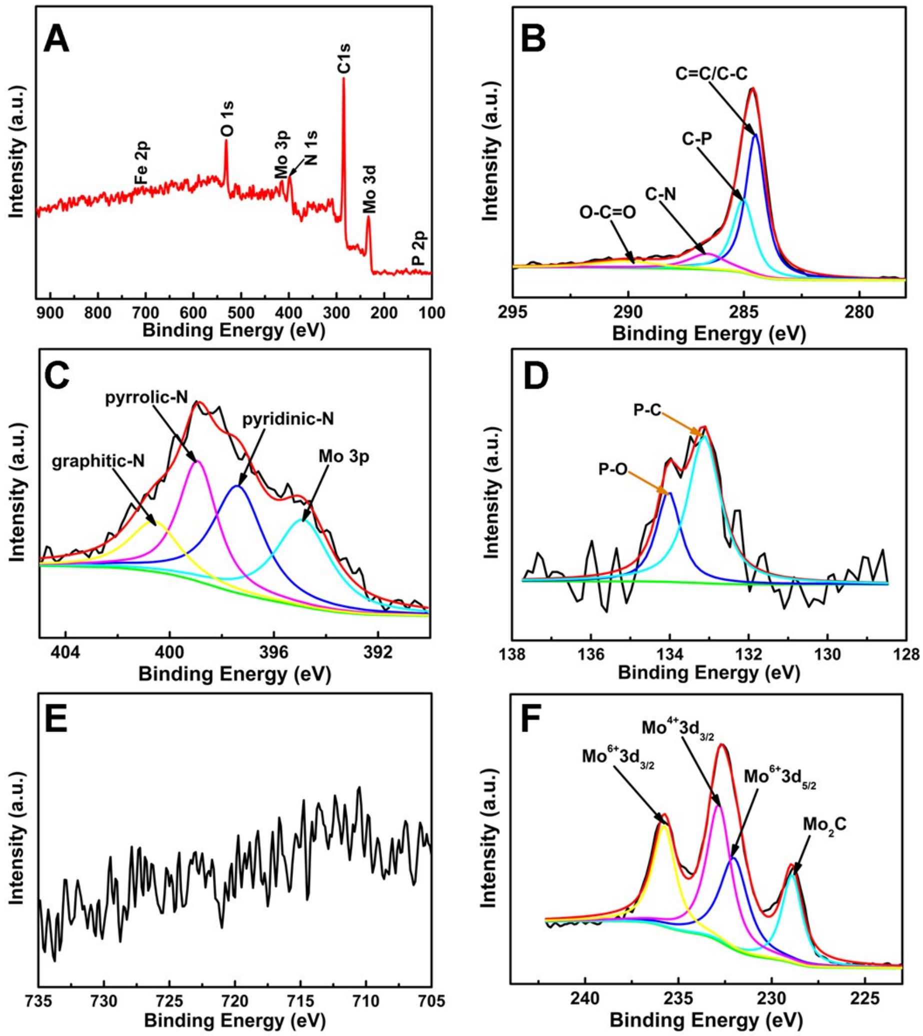

Fig. S16 (A-F) XPS survey spectra and high-resolution scans of C 1s, N 1s, P 2p, Fe 2p, and Mo 3d electrons of Fe_3C/Mo_2C@NPGC (1100 ^oC), respectively.

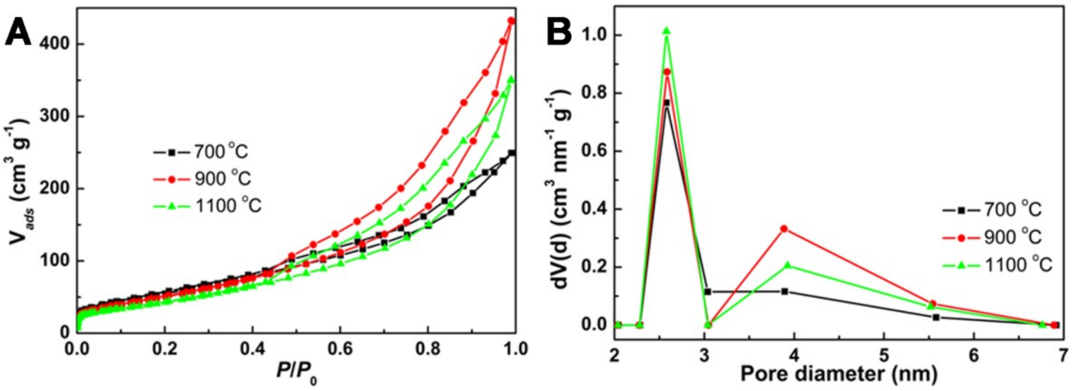

Fig. S17 N_2 adsorption-desorption isotherms (A) and (B) porous size distributions of different samples by BJH model.

S3. Tables in Supporting Information

Table S1. Atomic percents of different catalysts by XPS measurement and BET surface area.

catalysts	**C (at. %)**	**N (at. %)**	**O (at. %)**	**P (at. %)**	**Mo (at. %)**	**Fe (at. %)**	**BET surface area (m^2 g^{-1})**
Fe_3C@C	91.78		7.98			0.24	470
Fe_3C/FeMo/Mo_2C	29.34		50.58		14.26	5.82	40
Fe_3C/Mo_2C@NPGC-700	75.82	2.59	6.85	0.48	13.81	0.45	118
Fe_3C/Mo_2C@NPGC	73.03	1.82	10.3	0.37	14.06	0.42	128
Fe_3C/Mo_2C@NPGC-1100	73.87	1.5	10.45	0.25	13.93	0.38	120

Table S2 Comparison of the electrocatalytic activity of non-noble metal catalysts reported recently for HER

Catalyst	**Onset potential (mV)**	**Tafel slope (mV dec^{-1})**	**J_0 (A cm^{-2})[1]**	**η_{10} (mV)[2]**	**Ref.**
Fe_3C/Mo_2C@NPGC	**~18**	**45.2**	**1.04×10^{-4}**	**98**	**This work**
$NiMoN_x$/C	78	35.9	2.4×10^{-4}	~	*Angew. Chem. Int. Ed.*, **2012**, 51, 6131
MoC_x	25	53	2.3×10^{-5}	142	*Nat. Commun.* **2015**, 6, 6512
MoP-CA2	40	54	8.6×10^{-5}	125	*Adv. Mater.* **2014**, 26, 5702
P-WN/rGO	46	54	3.5×10^{-4}	85	*Angew. Chem. Int. Ed.* **2015**, 54, 6325
Mo_2C-RGO	70	57.3	~	130	*Chem. Commun.* **2014**, 50, 13135
Mo_2C/CNT-GR	62	58	6.2×10^{-5}	130	*ACS Nano*, **2014**, 8, 5163
Cu_3P NW/CF	62	67	1.8×10^{-4}	143	*Angew. Chem. Int. Ed.* **2014**, 53, 9577
Fe-WCN	100	~	~	220	*Angew. Chem. Int. Ed.* **2013**, 125, 13883
CoNi@NC	~0	104	~	142	*Angew. Chem. Int. Ed.* **2015**, 54, 2100
Mo1Soy-RGO	50	63	3.7×10^{-5}	109	*Energy Environ. Sci.* **2013**, *6, 1818*
MoCN	50	48	~	140	*J. Am. Chem. Soc.* **2015**, *137*, 110

Note: [1] represents the exchange current density, [2] represents the overpotential (η) at the current density of 10 mA cm^{-2},